First identification of ^{58}Zn β-delayed proton emission

A. A. Ciemny,[1,*] W. Dominik,[1] T. Ginter,[2] R. Grzywacz,[3,4] Z. Janas,[1] M. Kuich,[1] C. Mazzocchi,[1,†] M. Pfützner,[1] M. Pomorski,[1] D. Bazin,[2] T. Baumann,[2] A. Bezbakh,[5] B. P. Crider,[2] M. Ćwiok,[1] S. Go,[3] G. Kamiński,[5,6] K. Kolos,[3,7] A. Korgul,[1] E. Kwan,[2] S. Liddick,[2,8] K. Miernik,[1] S. V. Paulauskas,[2] J. Pereira,[2] T. Rogiński,[1] K. Rykaczewski,[4] C. Sumithrarachchi,[2] Y. Xiao,[3] H. Schatz,[2] and P. Sarriguren[9]

[1]*Faculty of Physics, University of Warsaw, 02-093 Warsaw, Poland*
[2]*National Superconducting Cyclotron Laboratory, Michigan State University, East Lansing, Michigan 48824, USA*
[3]*Department of Physics and Astronomy, University of Tennessee, Knoxville, Tennessee 37996, USA*
[4]*Oak Ridge National Laboratory, Oak Ridge, Tennessee 37831, USA*
[5]*Joint Institute for Nuclear Research, 141980 Dubna, Russia*
[6]*Heavy Ion Laboratory, University of Warsaw, 02-093 Warsaw, Poland*
[7]*Nuclear and Chemical Sciences Division, Lawrence Livermore National Laboratory, Livermore, California 94551, USA*
[8]*Department of Chemistry, Michigan State University, East Lansing, Michigan 48824, USA*
[9]*Instituto de Estructura de la Materia, Consejo Superior de Investigaciones Cientificas, Serrano 123, 28006 Madrid, Spain*

(Received 10 January 2020; accepted 28 February 2020; published 16 March 2020)

The β decay of ^{57}Zn and ^{58}Zn was investigated in an experiment at the National Superconducting Cyclotron Laboratory of Michigan State University. For the first time β-delayed proton emission from ^{58}Zn was observed with a branching ratio of 0.7(1)%. The proton-energy spectrum allowed for probing the Gamow-Teller strength distribution above the proton-separation energy in the daughter nucleus. Moreover, the absolute branching ration for delayed-proton emission from ^{57}Zn was found to be compatible with 100%.

DOI: 10.1103/PhysRevC.101.034305

I. INTRODUCTION

The region of the chart of nuclei close to the proton drip line offers unique opportunities to probe the properties of exotic nuclei with a large deficit of neutrons [1]. These nuclei are characterized by their large Q_β values and low proton-separation energies in the β-decay daughter, with consequent appearance of the β-delayed proton (βp) emission phenomenon. The study of βp emission from exotic nuclei gives the possibility to investigate the properties of proton-unbound excited states and the decay strength feeding them, since for these levels the competing γ-deexcitation path can be strongly hindered.

On the proton-rich side of the $N = Z$ line the isobaric analog state (IAS) in the β-daughter nucleus lies within the Q_β-value window. The β^+/EC decay of these exotic nuclei will therefore proceed mostly by a Fermi transition to the IAS, while a smaller portion of the β strength distribution will proceed via Gamow-Teller (GT) transitions to other states.

The reduced GT strength [B(GT)] distribution is an important observable both for understanding of nuclear structure away from stability and for astrophysical processes calculations, like those for the rapid proton-capture (rp) process [2–4]. While for most nuclei in the rp process the terrestrial ground-state half-lives have been measured, astrophysical applications require consideration of decays from thermally excited states and electron capture from free electrons in the astrophysical plasma. For these effects theoretical models have to be relied upon to provide the input data needed. While testing these models, verifying their capability to reproduce half-lives may not be sufficient, since different B(GT) distributions may give origin to the same half-life for the given nucleus. In order to test these models, it is desirable to collect as much information as possible on B(GT) distributions for the relevant nuclei. The GT strength distribution can be obtained directly by β-decay studies for the portion of the spectrum falling within the Q_β-value window. Complementarily to β-decay studies, B(GT) can be determined by charge-exchange (CE) reactions, at least in those cases for which a stable target is available [5]. Often, CE reactions are the only source of information available on B(GT) for particle-unbound states. The study the spectrum of β-delayed particle-emission of the β^+/EC precursor is an alternative way to gain knowledge on GT strength for particle-unbound states, that can readily be applied far from stability. The advantage of such approach when studying very exotic proton-rich nuclei is that large βp branching ratios ($b_{\beta p}$) are often observed and B(GT) above the proton-separation energy (S_p) can be investigated.

The study of neutron-deficient nuclei with $Z = 30$–40 can provide also important input for simulation of the thermonuclear runaway on the surface of accreting neutron stars (x-ray bursts) driven by rp process [6]. In particular, βp emission has been shown to affect the rp process powering astrophysical

*aleksandra.ciemny@fuw.edu.pl
†chiara.mazzocchi@fuw.edu.pl

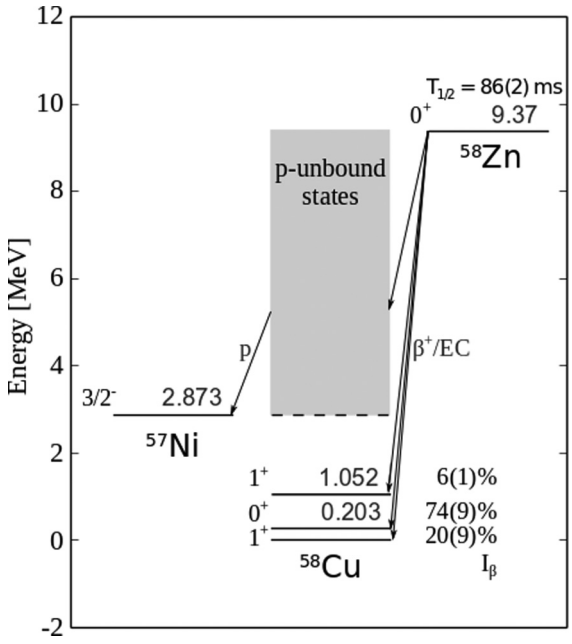

FIG. 1. Decay scheme of ^{58}Zn [9,10], see text for details. Energy values are given in MeV.

x-ray bursts [7]. ^{57}Zn and ^{58}Zn are both on the path of the rp process.

Direct identification and mass measurement of ^{58}Zn were performed with the pion double-charge exchange reaction ^{58}Ni(π^+,π^-) ^{58}Zn [8]. The β decay of ^{58}Zn was studied for the first time with the ISOL technique with selective laser ionization and its half-life was determined to be 86(18) ms. At the same time an upper limit for βp emission was set to 3% [9]. Later measurements confirmed the half-life with improved accuracy [86(2) ms] and the nonobservation of βp emission [10]. The decay of ^{58}Zn proceeds via a superallowed Fermi transition to the 0^+ first excited state in ^{58}Cu (IAS), at only 203 keV excitation energy, and via GT transitions to the ground state and to the 1^+ state at 1.052 keV [9,10]. Figure 1 shows the partial decay scheme of ^{58}Zn in which all data published to date is reported. Very small $b_{\beta p}$ values are expected, since the IAS, which draws most of the β-decay strength, lies below S_p in ^{58}Cu.

Absolute β feeding intensities (I_β) and B(GT) were determined in Ref. [10] for the three known states in ^{58}Cu, assuming no βp emission. However, the levels above S_p in ^{58}Cu are expected to play a non-negligible role in the B(GT) distribution and may have relevance in the rp-process framework.

The mirror nucleus of $^{58}_{30}Zn_{28}$ is $^{58}_{28}Ni_{30}$. Hence, assuming mirror symmetry, B(GT) transition strength to excited states in ^{58}Cu can be obtained by studying the ^{58}Ni$(^3$He$, t)$ ^{58}Cu reaction at intermediate energies [5,11,12]. The lowest-lying proton-unbound states have been investigated previously by means of ^{58}Ni(^{3}He, t) ^{58}Cu CE reactions in two experiments, that aimed at careful proton- [11] and γ-decay [12] study of the levels populated. High-energy-resolution measurements by Fujita *et al.* yielded a detailed mapping of the B(GT) distribution, in particular, in the first few MeV proton-energy region [11]. On the other hand, the study by Hara *et al.* [12] addressed also the γ-decay branch of the same levels, and established the branching ratio for the two competing decay modes up to 3.7 MeV ^{58}Cu excitation energy by means of proton-γ coincidences. Above this energy value no γ-decay competition was observed. These measurements show that there are several states above S_p populated with a B(GT) comparable to that for the proton-bound 1^+ excited state [11,12]. βp emission is therefore expected and its observation would provide data on higher-lying GT strength distribution with respect to previous β-decay measurements. This would be important information complementary to that provided by CE reactions, since in such studies background subtraction is particularly delicate, as concluded by Jokinen *et al.* in their work [9].

β-delayed proton decay of ^{57}Zn was studied first by Vieira *et al.* [13], who first observed three proton groups between 1.95 and 4.65 MeV. More recently Jokinen *et al.* [14] remeasured the delayed-proton energy spectrum with high resolution. In this measurement, relative branching ratios for the proton transitions to the ground and first excited states in ^{56}Ni were determined. In a 2007 work, Blank *et al.* [15] provided an updated reference value for the half-life.

Motivated by the above-mentioned considerations, a reinvestigation of the β decays of ^{57}Zn and ^{58}Zn was carried out. In this paper we report on the first observation of βp emission from ^{58}Zn and on the determination of the absolute total branching ratio for βp emission from ^{57}Zn.

II. EXPERIMENTAL TECHNIQUE

The experiment was performed at the National Superconducting Cyclotron Laboratory (NSCL) of Michigan State University (MSU). The details of the experiment were given in Refs. [16,17] and are summarized in the following. Neutron-deficient Zn and Ge isotopes were produced in fragmentation reaction of ^{78}Kr beam on a ^{nat}Be target and separated from the other reaction products by means of the A1900 separator [18]. They were later stopped in the Warsaw Optical Time Projection Chamber (OTPC) [19] that was placed at the end of the transmission line.

Each fragment was identified by the standard energy-loss (ΔE) and time-of-flight (ToF) measurement. The ion optics for the A1900 spectrometer was optimized for ^{59}Ge or ^{60}Ge in two separate settings [16]. Hardware gates were set to allow triggering the data acquisition system only by the optimised ions, i.e., ^{59}Ge or ^{60}Ge, and part of ^{57}Zn and ^{58}Zn, respectively, present in the cocktail beam. After each trigger, the beam was blocked for 100 ms to avoid subsequent implantations, while waiting for the decay. A summary of the measurement conditions for each isotope studied is given in Table I.

ΔE-ToF plots for all identified fragments reaching the detection setup and for ions triggering the data acquisition (DAQ) are shown in Fig. 2. They correspond to the ion-optics setting optimized for ^{60}Ge. More than 36000 (more than 500) events for which ^{58}Zn (^{57}Zn) triggered the DAQ and was

TABLE I. Ion optics settings of the A1900 spectrometer and the corresponding ion studied in this work. The number of implanted ions, half-life, and duration of the observation window (during which the beam was blocked at the source) are also given.

ion-optics setting	ion	No. impl. ions	$T_{1/2}$ (ms)	beam blocking (ms)
^{59}Ge	^{57}Zn	545	38(4) [14] 48(3) [15]	100
^{60}Ge	^{58}Zn	36339	86(2) [10]	100

implanted correctly into the detection setup were recorded during 2.5 (6.3) days of data taking.

The OTPC is a time-projection chamber with optical readout, which was filled with a gas mixture of 49.5% He + 49.5% Ar + 1% CO_2 at atmospheric pressure. Ions enter the active volume horizontally, perpendicularly to the electric drift-field lines, and are stopped in the gas where they subsequently decay. The ionization electrons generated by the ions and charged-particle decay-products drift towards the amplification stage, where they are multiplied by a set of four gas electron multiplier (GEM) foils, and light is generated. The photons are then detected by a CCD camera and a photomultiplier tube (PMT). After a trigger, the CCD camera exposition window is extended by 100 ms during which the PMT signal is recorded by means of a digital oscilloscope. The trajectory of the particle is reconstructed in three dimensions by combining the information stemming from the CCD image [projection on the xy plane) and PMT (time distribution of the signal, i.e., z component of the track after correction for the electron drift velocity, $v_{drift} = 1.05(2)$ cm/μs]. See Ref. [17] for details.

III. RESULTS AND DISCUSSION

A. ^{58}Zn

The analysis of the decay signals of over 36000 implanted ^{58}Zn ions yielded the first and unambiguous identification of 88 decays by delayed proton emission. Only events in which all ions entering the chamber were stopped in the active region of the detector were considered in the analysis. In Fig. 3, the

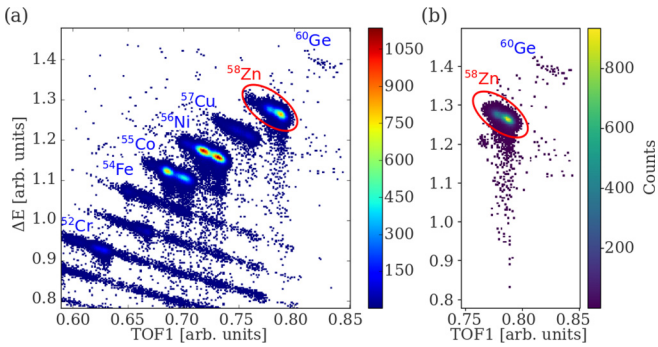

FIG. 2. ID-plot of (a) all fragments identified during the experiment and (b) triggering ions. Both plots refer to the ion-optics setting optimised for ^{60}Ge. See text for details.

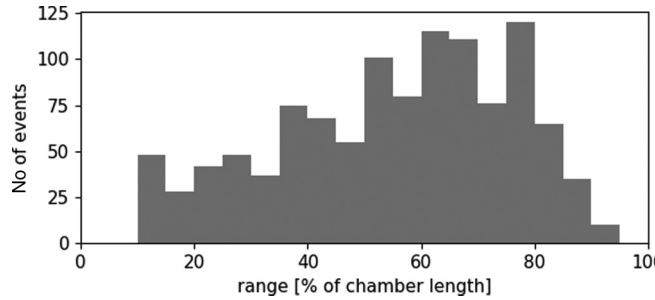

FIG. 3. Implantation profile of identified ^{58}Zn ions (events in which only a single ion entered the chamber, ≈3% of the total statistics). The abscissa shows the depth into the chamber along the beam direction. Only ions implanted within 10 and 90% of the chamber length were considered further in the analysis.

implantation profile of ^{58}Zn ions in the chamber is shown. The assignment of the delayed-proton events to the decay of ^{58}Zn is supported by the fact that the decay products (βp) are correlated in time and space with an implanted ^{58}Zn ion. Moreover, with the exception of ^{60}Ge, which is a known βp emitter [17], all other isotopes in the cocktail beam, which enter the chamber and are recorded in the same event, are less exotic. Among them, only ^{57}Cu has a positive Q value for βp emission, but the energy window for this decay mode is rather small (1443 keV [20]) and its half-life long with respect to the observation window [$T_{1/2}(^{57}\text{Cu}) = 196.3$ ms, giving a probability of 30% to observe a ^{57}Cu decay event]. The amount of ^{57}Cu contaminants was at the level of 0.15 ^{57}Cu ions for each ^{58}Zn event. Combining all this information, for each ^{58}Zn event, we expect to have 0.05 delayed protons from ^{57}Cu assuming $b_{\beta p} = 100\%$. For comparison ^{58}Zn has about 4 times higher $Q_{\beta p}$ and the same calculation yields 7 times larger probability to observe βp from ^{58}Zn assuming $b_{\beta p} = 100\%$.

Example βp events from ^{58}Zn, in which protons are stopped in the detector, are displayed in Fig. 4. The other ions visible in the CCD images were all identified as belonging to the nontriggering, less exotic fragments.

The analysis of the PMT waveform shapes indicates that most of the registered protons were emitted downwards. This points to the fact that ^{58}Zn ions are not fully neutralized in the gas mixture and drift towards the cathode before decaying, as described in Ref. [17]. The drift time from the implantation point to the electrode for the ions is 20(5) ms. During this time the detector is therefore sensitive to protons emitted into the full solid angle. As the ions reach the cathode, the detection efficiency drops to 50%. Taking this into account, as well as the limited detection time window with respect to the half-life, the amount of protons emitted from the implanted ^{58}Zn ions that could be detected is 35(3)% as determined from the formula

$$\frac{1}{\tau}\left(\int_{100\mu s}^{20ms} e^{-t/\tau}dt + \frac{1}{2}\int_{20ms}^{86ms} e^{-t/\tau}dt\right),$$

with τ the lifetime. The resulting branching ratio for βp emission was calculated to be 0.7(1)%. This value is compatible with the upper limit of 3% given by Jokinen *et al.* [9].

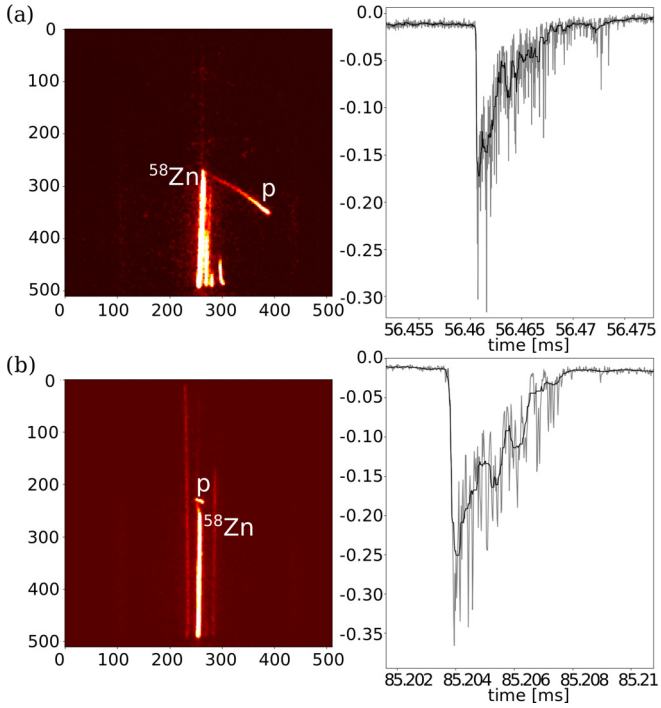

FIG. 4. (a) and (b) Example CCD pictures (left) and respective fragments of the PMT signal corresponding to the proton track (right) collected during the experiment. The gray histogram shows the raw PMT signal, while the black curve is the same signal processed through a median filter. The decision on whether a proton is stopped inside the chamber or not is based on the observation of the Bragg peak in the CCD image rather than in the PMT signal because of the noise levels in the latter. See text for details.

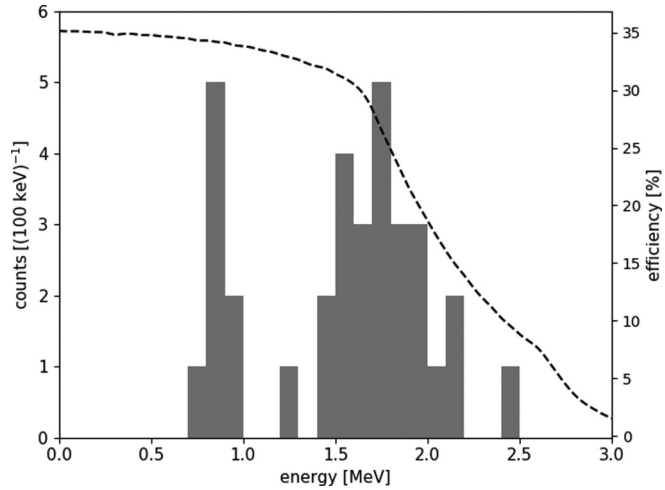

FIG. 5. Energy spectrum of the 33 reconstructed ^{58}Zn βp events. The proton-stopping efficiency as a function of the energy, under the assumption that the ions are drifting, is shown with a black dashed line. See text for details.

Among the 88 protons observed, 55 escaped the chamber and could not be considered further in the analysis. The energies of the stopped protons were estimated on the basis of the duration of the PMT signal, the trajectory in the CCD image, and the energy dependence of the range for protons in the gas mixture used, calculated with the SRIM code [21]. The energy spectrum is displayed in Fig. 5. The detector, in the configuration used, allows for observation of protons with energies as low as 200–400 keV. Nevertheless, all the protons observed had an energy larger than 700 keV. The upper energy limit of the spectrum is due to the fact that protons with longer ranges (higher energies) escape the chamber. The exact limit depends on the emission angle and on when the decay happened with respect to the ion drift towards the cathode. The efficiency for detecting a stopped proton is plotted on the energy spectrum in Fig. 5 as a function of proton energy, highlighting the region of the spectrum where not all protons may be stopped in the chamber. A group of proton events at ≈0.85 MeV ($E_x \approx 3.75$ MeV) is present, indicating the possible existence of one or more peaks. An example of a proton belonging to this portion of the spectrum, with energy 0.79(4) MeV, is presented in Fig. 4(b). Another group of proton lines from ≈1.4 to ≈2.2 MeV can be identified. They correspond to excitation energies between ≈4.3 and ≈5.1 MeV in ^{58}Cu, respectively, assuming decay to the ground state of ^{57}Ni. The energy resolution does not allow to determine better their energy, nor resolving further the transitions originating each of them. The proton groups identified in this work are in agreement with the expectations from CE studies reported in Ref. [11], see Table II.

The proton-energy spectrum determined in this work allows us to investigate the region of ^{58}Cu excitation energies between ≈3.4 and ≈5.2 MeV. The group at 0.85 MeV most likely corresponds to the decay of the 3.678 and 3.717 MeV 1^+ states in ^{58}Cu. Despite the low resolution, it is clear that the 3.460 MeV level does not appear to deexcite by βp emission, while it shows the largest GT strength for population in the ^{58}Ni(^{3}He, t) CE reaction. It is important to note that the 3.678 MeV state has a significant γ-decay branch (85(17)% [12,22]), although affected by a large uncertainty. Both the 3.460 and 3.678 MeV levels have recently been observed in β-delayed γ-ray decay of ^{58}Zn with a significant branching [23]. Since the present data do not allow us to disentangle the contribution by the individual states to the proton group, the branching ratios, and therefore the B(GT), determined in the following are only lower limits on their respective value. The group of proton lines between ≈1.4 and ≈2.2 MeV ($E_x = 4.3$–5.1 MeV) corresponds likely to the 4.720 MeV 1^+ state and the unresolved 5.065 and 5.160 MeV 1^+ levels in ^{58}Cu. In the following this group of lines is subdivided into two parts, a more intense one around 1.75 MeV and the other, smaller group, centered around 2.1 MeV.

On the basis of the observed number of protons and considerations reported above, we have calculated the branching ratios for the proton groups at ≈0.85, ≈1.75, and ≈2.1 MeV ($E_x =\approx 3.75$, ≈4.65, and ≈5.0 MeV, respectively), using the curve shown in Fig. 5 for the energy-dependent efficiency. We have estimated the B(GT) corresponding to the feeding of low-lying proton-unbound states in ^{58}Cu. The results are summarized in Table II. Despite the small branching ratio, the B(GT) strength for the proton-unbound levels is comparable in intensity to the value of 0.17(3) obtained by Kucuk *et al.*

TABLE II. Energies and branching ratios for low-lying 1^+ states in ^{58}Cu. GT strength determined from CE reactions and β decay is given. The branching ratios for βp emission from ^{58}Zn are not corrected for the γ-decay probability.

β decay of ^{58}Zn				^{58}Ni(^{3}He, t) ^{58}Cu CE reaction				
E_x MeV	$b_{\beta p}$ %	B(GT)	Ref.	E_x MeV	B(GT)	Ref.	$b_{\beta p}$ %	Ref.
0	0	0.30(13)	[10]	0	0.155(1)	[25]		
1.051	0	0.17(3)	[10]	1.051	0.265(13)	[11]		
				2.949	0.025(3)	[11]		
				3.460	0.173(11)	[11]	62(11)	[12]
≈3.75	⩾0.06(2)	⩾0.015(8)	this work	3.678	0.155(10)	[11]	15(17)	[12]
				3.717	0.050(5)	[11]	100%	[12]
≈4.65	0.20(6)	0.13(6)	this work	4.720	0.042(4)	[11]	100%	[12]
				5.065	0.040(4)	[11]	100%	[12]
				5.160	0.250(14)	[11]	100%	[12]
≈5.0	0.05(3)	0.05(4)	this work		0.290(6)			

[10] for the 1051 keV 1^+ state in ^{58}Cu in their recent β-decay work. βp emission should therefore not be neglected when looking at B(GT) distribution, even when its probability is very small. The level at 3.460 MeV observed with significant B(GT) strength in Ref. [11] does not appear to decay by βp emission, while the two levels at 3.69 and 3.72 MeV draw a much smaller strength with respect to the CE reaction measurement [11].

We have analyzed the results in the framework of QRPA approach based on self-consistent deformed Hartree-Fock mean field with Skyrme forces [2]. The calculations reported in Ref. [2], which correspond to a spherical solution for ^{58}Zn, use the Skyrme SLy4 interaction [24]. They give pronounced peaks of the GT strength below 2.5 MeV and above 7 MeV, but practically nothing between 4 and 6 MeV. A spherical approximation seems to be justified in the case of ^{58}Zn, since it lies only two protons above the doubly magic ^{56}Ni nucleus. The energy distribution of the GT strength can therefore be understood in terms of transitions between spherical shells. Nevertheless, deformation and pairing effects will induce some fragmentation of the GT strength because of the energy splitting of the spherical levels and the partial occupation of the states. Reducing the pairing interaction causes the increase of the equilibrium-configuration deformation to values of about $\beta = -0.1$. Despite being still quite small, such deformation causes an enhancement of the GT strength at excitation energies around 5 MeV (see Fig. 6), in the region where the experimental strength is found, and therefore was included in the calculations.

The analysis of the GT strength distribution shows that the contributions coming from deformed states originating in spherical shells with different orbital angular momentum L, are enhanced with respect to the spherical case, where these states are not connected by the GT operator. These deformed states mix different L values and generate non-negligible matrix elements. In particular, the strength at around 5 MeV is caused by transitions between deformed states that, in the spherical limit, correspond to $\pi f_{7/2} \rightarrow \nu p_{3/2}$ and $\pi p_{3/2} \rightarrow \nu f_{5/2}$. This approximate analysis allows to extract the main properties of the transitions involved in the process:

$E_x(^{58}\text{Cu}) = 0$–1 MeV $\quad \pi p_{3/2} \rightarrow \nu p_{3/2}$
$E_x(^{58}\text{Cu}) = 2.5$–$3$ MeV $\quad \pi p_{3/2} \rightarrow \nu p_{1/2}$
$E_x(^{58}\text{Cu}) = 4$–5 MeV $\quad \pi f_{7/2} \rightarrow \nu p_{3/2}$ and $\pi p_{3/2} \rightarrow \nu f_{5/2}$
$E_x(^{58}\text{Cu}) = 6.5$–$7$ MeV $\quad \pi f_{7/2} \rightarrow \nu p_{1/2}$
$E_x(^{58}\text{Cu}) > 7$ MeV $\quad \pi f_{7/2} \rightarrow \nu f_{5/2}$

All of the main transitions occur from highly occupied proton states to almost empty neutron states. The strength in the regions with $E < 3$ MeV and $E > 7$ MeV (transitions between states with the same L) is rather large, while the strength in regions with 4 MeV $< E <$ 7 MeV is not as large because

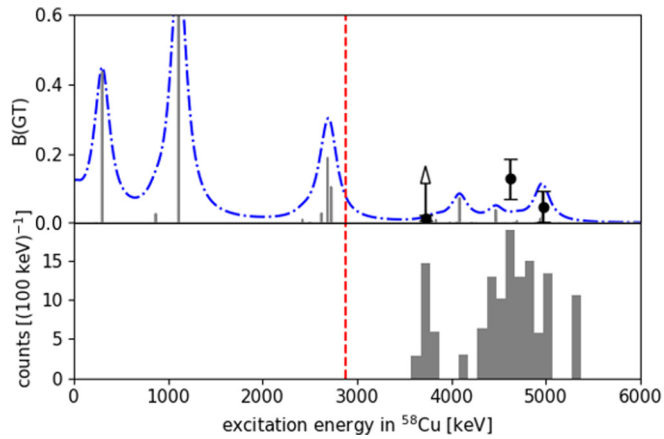

FIG. 6. (Top) B(GT) values for decay of ^{58}Zn from experiment for $E_x > S_p$ (full circles with error bars, this work) and from QRPA calculations (see text for details) up to 6 MeV excitation energy. The gray bars show the B(GT) calculations, while the dash-dotted blue line represents the calculated B(GT) folded with 0.2 MeV-wide Breit-Wigner distributions to account for the energy resolution. The vertical dashed line shows the S_p value in ^{58}Cu. (Bottom) Energy spectrum of βp from ^{58}Zn decay reported on the excitation-energy scale for comparison with the calculations. The spectrum has been corrected for the efficiency (see Fig. 5).

of the different dominant L values, but it is still sizable since it comes from transitions between deformed states with many different L values involved. Therefore, within this approach, effects induced by deformation generate the strength between 3 and 7 MeV observed in the experiment.

We investigated the impact of β-delayed proton emission of ^{58}Zn on the rp process using a one zone x-ray burst model [26,27]. While ^{58}Zn is on the path of the rp process, the impact of βp emission on energy generation and burst light curve is negligible because the β daughter ^{58}Cu and the βp daughter ^{57}Ni are in (p, γ)-(γ, p) equilibrium with each other for most of the conditions where the rp process operates in this mass region. However, the final $A = 57$ abundance in the burst ashes is affected by late time βp decay of ^{58}Zn. A branch of 100% would increase the final $A = 57$ abundance by a factor of 3–4, with final abundances up to 2×10^{-5} depending on the burst model. The $A = 57$ abundance may affect Urca cooling in the neutron star crust, where $A = 57$ nuclei have been shown to exhibit strong cooling [28]. However, both the 0.7% branch measured here and the previous upper limit of 3%, only change the final abundance by a few %, which is negligible.

B. ^{57}Zn

The decays of 545 implanted ^{57}Zn ions were analyzed in this work. From the 325 decays by proton emission observed, a half-life of 27(3) ms was determined, in agreement within 2σ with 38(4) ms from Ref. [14] and 40(10) ms from Ref. [13], but not with 48(3) ms [15]. A weighted average of the four results gives 38(2) ms. Taking the detection efficiency into account [66(7)%], it was possible to determine the total branching ratio for the βp decay channel, $b_{\beta p} = 90(10)\%$, in agreement with the previous value of 78(17)% [15], both consistent with 100%. The reconstruction of the energy for those protons that are stopped into the chamber shows a spectrum characterized by much lower-energy resolution than the one determined in Ref. [14], but consistent with it. Moreover, the branching ratios can be determined accurately, since the identification of the proton events is not affected by the resolution. The larger branching will make it more difficult for the rp process to bypass the ^{56}Ni waiting point. However, for firm conclusions a more precise branching would have to be determined.

IV. SUMMARY

β decay of ^{58}Zn was investigated in an experiment performed at the NSCL of MSU by means of the OTPC detector. The first measurement of βp emission from this nucleus was performed. Its branching ratio and the partial delayed-proton energy spectrum were established. Despite $b_{\beta p}$ being only 0.7(1)%, the measurement of the proton energy distribution allowed to study the B(GT) distribution to states just above the proton separation energy in the ^{58}Cu daughter. A comparison of the results with QRPA calculations indicated that the β-decay strength feeding proton-unbound states in the daughter nucleus is generated by effects induced by deformation. The results have been discussed also within the framework of the astrophysical rp process. The change in the final abundances due to the βp branch of ^{58}Zn was found to be negligible. Higher statistics and complementary measurements allowing to study the full range of the proton spectrum with good resolution are needed, in order to fully probe the B(GT) distribution above the proton-separation energy. Moreover, the β decay of ^{57}Zn was investigated and its absolute branching ratio for decay by βp emission was found to be consistent with 100%.

ACKNOWLEDGMENTS

We wish to acknowledge the National Superconducting Cyclotron Laboratory staff for assisting with the experiments and providing excellent quality radioactive beams. Operation of the NSCL was supported by the National Science Foundation under Grant PHY-1102511. This work was supported by the National Science Center, Poland, under Contract No. UMO-2015/17/B/ST2/00581, by the US Department of Energy, Office of Science, Office of Nuclear Physics, under US DOE Grants No. DE-AC05-00OR22725 (ORNL) and No. DE-FG02-96ER40983 (UTK), by the fund source National Nuclear Security Administration Grant No. DEFC03-03NA00143, and under the Stewardship Science Academic Alliance program through DOE Cooperative Agreement No. DE-FG52-08NA28552 (UTK). A.A.C. acknowledges support by the Polish Ministry of Science and Higher Education through Grant No. 0079/DIA/2014/43 (”Grant Diamentowy”). H.S. acknowledges support by the US National Science Foundation under awards PHY-1430152 (JINA Center for the Evolution of the Elements) and PHY-1102511. P.S. acknowledges support from MCIU/AEI/FEDER_UE (Spain) under Grant No. PGC2018-093636-B-I00.

[1] M. Pfützner, M. Karny, L. V. Grigorenko, and K. Riisager, Rev. Mod. Phys. **84**, 567 (2012).
[2] P. Sarriguren, Phys. Rev. C **83**, 025801 (2011).
[3] E. Caurier, K. Langanke, G. Martínez-Pinedo, and F. Nowacki, Nuclear Physics A **653**, 439 (1999).
[4] T. Suzuki, M. Honma, T. Otsuka, and T. Kajino, JPS Conf. Proc. **6**, 020029 (2015).
[5] Y. Fujita, B. Rubio, and W. Gelletly, Prog. Part. Nucl. Phys. **66**, 549 (2011).
[6] W. Lewin, J. von Paradijs, and R. Taam, Space Sci. Rev. **62**, 223 (1993).
[7] G. Lorusso *et al.*, Phys. Rev. C **86**, 014313 (2012).
[8] K. K. Seth, S. Iversen, M. Kaletka, D. Barlow, A. Saha, and R. Soundranayagam, Phys. Lett. B **173**, 397 (1986).
[9] A. Jokinen *et al.*, Eur. Phys. J. A **3**, 271 (1998).
[10] L. Kucuk *et al.*, Eur. Phys. J. A **53**, 134 (2017).
[11] Y. Fujita *et al.*, Eur. Phys. J. A **13**, 411 (2002).
[12] K. Hara *et al.*, Phys. Rev. C **68**, 064612 (2003).

[13] D. J. Vieira, D. F. Sherman, M. S. Zisman, R. A. Gough, and J. Cerny, Phys. Lett. B **60**, 261 (1976).
[14] A. Jokinen *et al.*, EPJdirect A **3**, 1 (2002).
[15] B. Blank *et al.*, Eur. Phys. J. A **31**, 267 (2007).
[16] A. A. Ciemny *et al.*, Phys. Rev. C **92**, 014622 (2015).
[17] A. A. Ciemny *et al.*, Eur. Phys. J. A **52**, 89 (2016).
[18] D. J. Morrissey *et al.*, Nucl. Instr. Meth. Phys. Res. B **204**, 90 (2003).
[19] M. Pomorski *et al.*, Phys. Rev. C **90**, 014311 (2014).
[20] M. Wang, G. Audi, F. G. Kondev, W. J. Huang, S. Naimi, and X. Xu, Chin. Phys. C **41**, 030003 (2017).
[21] www.srim.org
[22] C. D. Nesaraja, S. D. Geraedts, and B. Singh, Nuclear Data Sheets **111**, 897 (2010).
[23] https://www.jstage.jst.go.jp/article/jpsgaiyo/72.2/0/72.2_253/_pdf/-char/ja
[24] E. Chabanat, P. Bonche, P. Haensel, J. Meyer, and R. Schaeffer, Nucl. Phys. A **635**, 231 (1998).
[25] B. Singh, Nuclear Data Sheets **87**, 177 (1999).
[26] H. Schatz, A. Aprahamian, V. Barnard, L. Bildsten, A. Cumming, M. Ouellette, T. Rauscher, F.-K. Thielemann, and M. Wiescher, Phys. Rev. Lett. **86**, 3471 (2001).
[27] R. H. Cyburt *et al.*, Astroph. J. **830**, 55 (2016).
[28] H. Schatz *et al.*, Nature (London) **505**, 62 (2014).